



Pergamon

Bioorganic & Medicinal Chemistry Letters 11 (2001) 2631–2635

BIOORGANIC &
MEDICINAL
CHEMISTRY
LETTERS

Design, Synthesis and Characterisation of a Peptide with Oxaloacetate Decarboxylase Activity

Susan E. Taylor, Trevor J. Rutherford[†] and Rudolf K. Allemann*

The University of Birmingham, School of Chemistry, Edgbaston, Birmingham, B15 2TT, UK

Received 11 May 2001; revised 10 July 2001; accepted 25 July 2001

Abstract—The synthesis of Oxaldie-3, a synthetic 31-residue peptide with oxaloacetate decarboxylase activity, is described. Bio-physical characterisation by gel filtration, CD and NMR spectroscopy indicated that the peptide adopted a folded structure in solution. Oxaldie-3 was an efficient catalyst at concentrations as low as 2 μ M, 100-fold lower than the previously described Oxaldie-2, which relied on aggregating α -helices for activity. Oxaldie-3 speeded decarboxylation by more than three orders of magnitude relative to simple amines. © 2001 Elsevier Science Ltd. All rights reserved.

Biological macromolecules of defined structure and with catalytic activity can be created through selection of a few catalytically active biomolecules from a large pool of randomly generated, mainly inactive molecules^{1–4} or by rational design of biomolecules that fold in solution to present to the substrate an array of catalytic functional groups.^{5–7} The success of designing polypeptide catalysts is a vigorous test of our understanding of protein folding and enzyme catalysis.⁸

In the present investigation we report the design, synthesis and characterisation of an unnatural oxaloacetate decarboxylase. While all natural oxaloacetate decarboxylases depend on metal catalysis, the decarboxylation of acetoacetate by acetoacetate decarboxylase is speeded up by an active site lysine with a pK_a of approximately 6, 4 orders of magnitude lower than the side chain of an unperturbed lysine.^{9,10} Acetoacetate decarboxylase accomplishes this remarkable reduction in the pK_a by placing a second amino group close to the reactive lysine in the active site.¹¹ Based on a general understanding of the amine-catalysed decarboxylation of beta-keto acids, a reaction that proceeds through a protonatable imine intermediate, we previously reported the construction of a peptide with oxaloacetate decarboxylase activity (Oxaldie-2).^{5,12,13} Oxaldie-2 folded into an amphiphilic α -helix, where one side of the helix was hydrophilic and the other hydrophobic. These amphiphilic helices formed helical bundles in aqueous

solution and served as the scaffolding for holding a reactive amine. Proper folding and catalytic activity of Oxaldie-2 were concentration dependent. Above concentrations of 200 μ M, where Oxaldie-2 was fully helical, imine formation between oxaloacetate and the active amine of Oxaldie-2 was speeded by 2–3 orders of magnitude relative to simple amines.⁵ Attempts to identify better catalysts by screening a combinatorial library of an 18-amino acid peptide based on the sequence of the Oxaldie-2 led to a further rate enhancement of not even half an order of magnitude relative to Oxaldie-2,^{14,15} indicating that the simple design of Oxaldie-2 could not be improved much further. However, these results also stressed the remarkable success of de novo design, which at least in the case of Oxaldie-2 could compete with combinatorial approaches.

The catalytic activity of Oxaldie-2 was dependent on the high concentrations necessary for the formation of the helical bundles. Here we report the design, synthesis and characterisation of Oxaldie-3, a 31-amino acid residue polypeptide, which forms a stable structure in solution and acts as an efficient catalyst for the decarboxylation of oxaloacetate over a wide range of peptide concentrations.

Design and Synthesis of Peptide Scaffold

In order to create an enzyme with increased specific oxaloacetate decarboxylase activity the catalytically active amine was introduced into the scaffold of avian pancreatic polypeptide to create Oxaldie-3 (Fig. 1). Pancreatic polypeptides (PP) are single chain peptides of 36 amino acids.¹⁶ An X-ray structure of avian PP (aPP)

*Corresponding author. Tel.: +44-121-414-4359; fax: +44-121-414-4446; e-mail: rk Allemann@chemistry.bham.ac.uk

[†]Present address: MRC-Centre for Protein Engineering, Hills Road, Cambridge, CB2 2QH, United Kingdom.

at 1.4 Å and a solution structure of PP from cow are available.^{17–19} Despite their small size, PPs adopt a globular conformation which comprises of a proline-rich type II helix (residues 1–8) and an α -helix (residues 14–32) (Fig. 2). Residues 33–36, which are thought to be important for the biological activity of the peptides, are in an unordered conformation in solution and are not necessary for the formation of the three-dimensional structure. The two helices, which are joined by a type II beta-turn, interact through hydrophobic contacts to form a compact and stable tertiary structure. Further hydrophobic contacts in aPP are formed between subunits to form a stable dimer with a dissociation constant of approximately 100 nM.²⁰ In the design of Oxalide-3

the active site lysines were introduced on the solvent exposed face of the α -helix of aPP by replacing Ile (18), Asp (22), Gln (25) and Asn (29) (Fig. 1). Therefore the hydrophobic core between the α -helix and the proline-rich helix as well as the interactions between the subunits of the protein dimer are not affected. To stabilise the helices, the N-terminal amine of Oxalide-3 was acetylated and the carboxy-terminus designed as an amide.

Oxalide-3 was synthesised by solid-phase peptide synthesis using Fmoc chemistry and purified by reversed phase HPLC. The mass of Oxalide-3 was determined by MALDI-TOF and electrospray mass spectrometry as 3612, which matches the calculated mass.

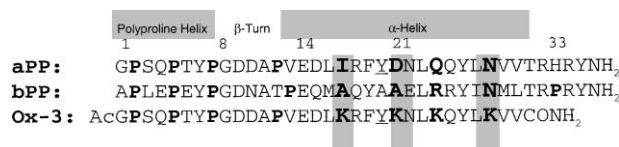


Figure 1. Sequence alignment of Oxalide-3 and avian and bovine pancreatic polypeptides. The proline-rich type II helix and the α -helical region are indicated. The residues, which were substituted by lysines, are indicated in bold.

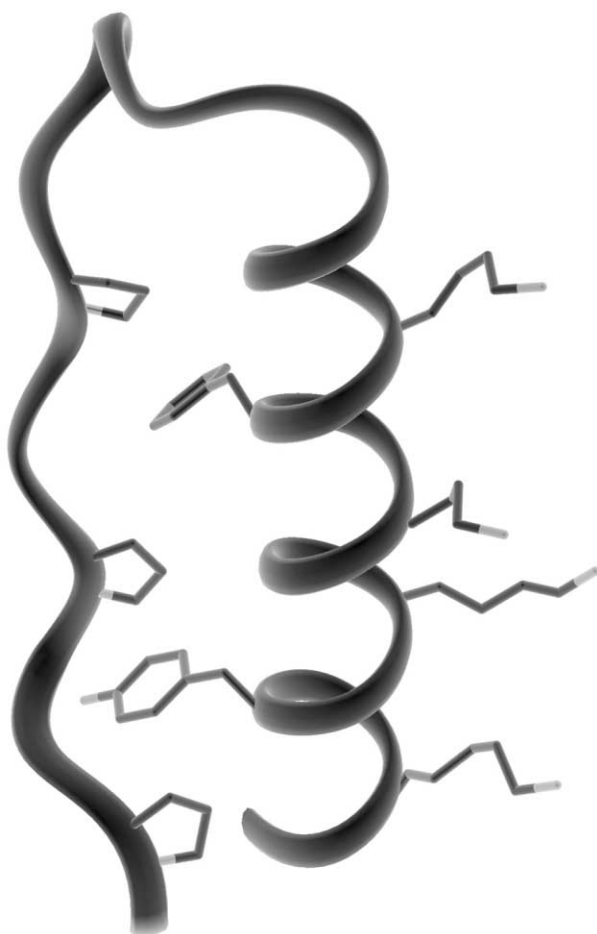


Figure 2. The structure of Oxalide-3 showing the positions of the lysine residues on the surface of the α -helix. The proline residues and the aromatic amino acids important for the stability of the folding unit are indicated. The model was based on the X-ray structure of aPP.¹⁷

Structural Characterisation of Oxalide-3

Gel filtration at peptide concentrations of 6.3 mM and 155 μ M through Sephadex G50 in 50 mM potassium phosphate (pH 7) and 10 mM NaCl revealed an apparent molecular weight for Oxalide-3 of \sim 8600 by comparison with the retention times of vitamin B12, bPP (1–31), α -lactalbumin, myoglobin, trypsin, and pepsin. Like wild-type aPP and bPP,²⁰ Oxalide-3 appeared to be dimeric under these conditions.

The circular dichroism spectrum of Oxalide-3 (1 mM potassium phosphate, pH 7, 10 mM NaClO₄) at room temperature showed that significant amounts of the peptide were in an α -helical conformation (Fig. 3). The spectrum compared well with that reported for wild-type aPP.²¹ From the ellipticity at 222 nm of $-19,877$ deg cm² dmol⁻¹, Oxalide-3 was calculated to be 52% α -helical.²² In the crystal structure of aPP 58% of the residues are in a helical conformation.¹⁷ Contrary to Oxalide-2, the molar ellipticities in the far UV circular dichroism spectrum of Oxalide-3 were independent of peptide concentration between 1 and 200 μ M.

The near UV CD spectrum of Oxalide-3 at 4.5 mM peptide concentration showed a doublet characteristic of a tyrosine residue (Fig. 3). Tyrosine (21) of aPP is located at the edge of the dimer interface where it makes a close asymmetric contact with the equivalent tyrosine in the second subunit.^{17,18} These tyrosines at the dimer interface of aPP have been identified as the likely source of the strong CD signals around 280 nm.

The thermal denaturation of Oxalide-3 was monitored by measuring the temperature dependence of the CD spectrum (Fig. 3). Isodichroic points were observed at 204 and 238 nm, suggesting a two-state equilibrium. Plotting the CD signal as a function of temperature revealed a clear plateau for the CD signal at high temperatures (Fig. 3). At the low temperature end the levelling off of the CD signal was less pronounced. However, the shape of the melting curve was sigmoidal and a melting temperature of 34°C was estimated by curve fitting. Flat melting curves are typical for small globular proteins because the folding transition shows relatively little co-operativity. On the other hand, the

flatness of the melting curve could also be interpreted as a gradual decrease in the helical content with increasing temperature as is typically observed for molten globules.

^1H - ^1H TOCSY, HSQC and HMQC-TOCSY NMR spectra enabled the assignment of many ^1H resonances for the individual amino acids, although the spectral dispersion was insufficient to fully resolve the spin systems of amino acids of the same type and obtain

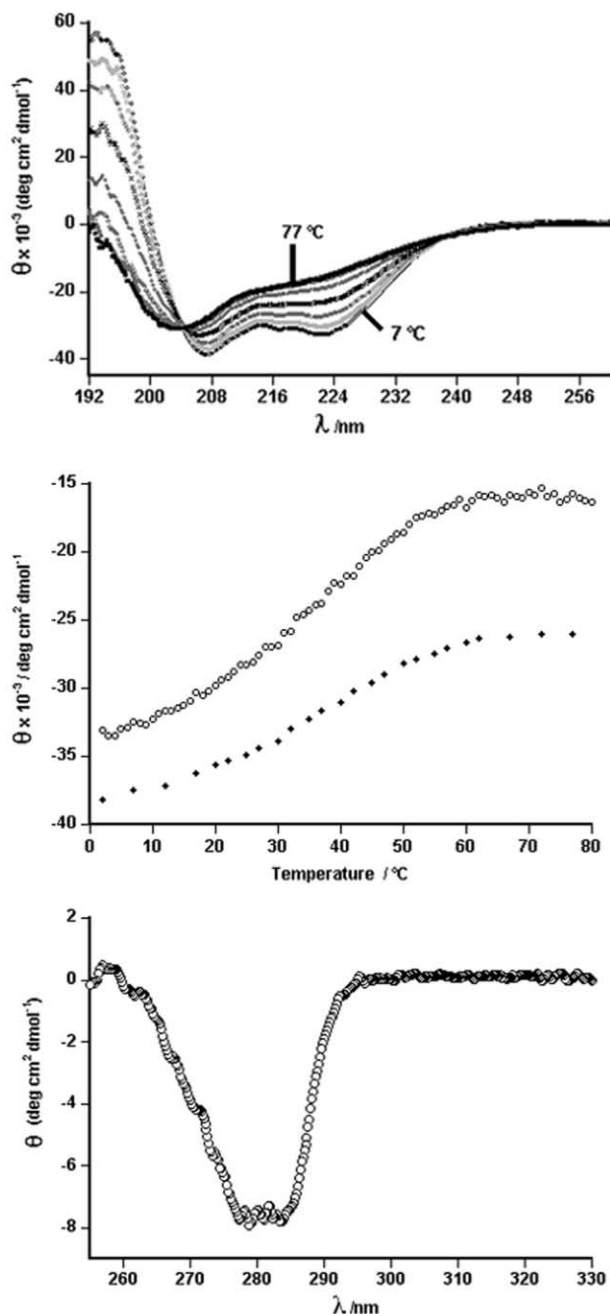


Figure 3. Top: thermal denaturation of 20 μM Oxaldie-3 in 1 mM potassium phosphate (pH 7) and 10 mM NaClO_4 as monitored by CD spectroscopy. Temperature increments are 10°C starting at 7°C . Middle: molar ellipticities at 208 (filled squares) and 222 (open octagons) nm of a 20 μM solution of Oxaldie-3 as a function of temperature (1 mM potassium phosphate (pH 7), 10 mM NaClO_4). Bottom: near UV CD spectrum of 4.5 mM Oxaldie-3 in 1 mM potassium phosphate (pH 7) and 10 mM NaCl.

sequence specific assignments. The side chain resonances of the 3 leucine, 3 valine and 4 lysine residues, for example, were only poorly resolved (Fig. 4). The lack of spectral dispersion and the random coil-like chemical shifts indicated that Oxaldie-3 did not adopt the same stable tertiary fold in solution as bPP.²³ However, NOESY cross-peaks depicting strong inter-residue NOEs indicated the presence of defined secondary structure (Fig. 5). For example, strong NOEs between the side chain resonances of tyrosine and leucine residues were taken as evidence that Oxaldie-3 did not adopt a random coil conformation. Weak NOEs between backbone amide protons were consistent with α -helical structure. Weak NOE cross peaks were also observed for the side chain stacking interactions between proline and tyrosine and/or phenylalanine residues. Spectra recorded for a separate sample of Oxaldie-3 at 30°C , at 4°C with 5% trifluoroethanol as the cosolvent, and at 4°C in the presence of 150 mM NaCl showed similar low dispersion of signals. Minor ^1H chemical shift perturbations gave rise to a significantly different appearance of the one-dimensional ^1H spectrum. Comparison of TOCSY spectra at 4 and 30°C , however, revealed that the shift changes were relatively minor, indicating no substantial restructuring of the polypeptide. The ^1H NMR spectra, therefore, exhibited the characteristics of a molten globule state observed for partially folded polypeptides, with ^1H chemical shifts closer to those of a random coil than to those of a folded state.²⁴ The molten globule state is characterised by a compactness similar to that of the native state with native-like secondary structure and a fluctuating tertiary structure resulting from non-rigid side chain packing.²⁵

The formation of a molten globule-like state of Oxaldie-3 can have two reasons. Either the introduction of the 4 lysines on the solvent exposed face of the α -helix of aPP destabilised the native folded form of Oxaldie-3 or aPP does not adopt the same conformation in solution as in the crystalline state. Residues 18, 22, 25 and 29 of aPP, which were replaced with lysines in Oxaldie-3, are not involved in interactions between the α -helix and the

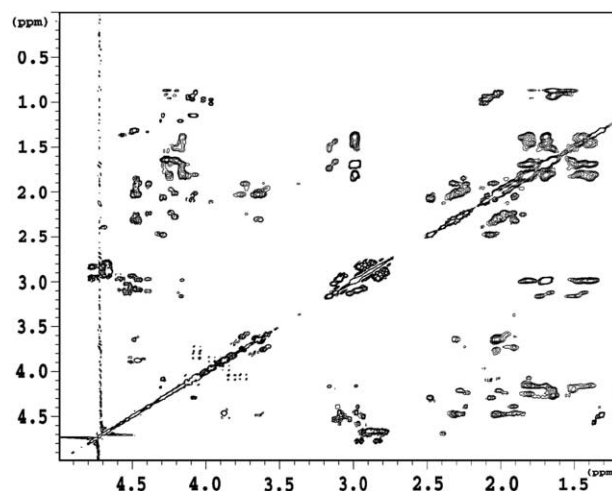


Figure 4. 500 MHz ^1H - ^1H TOCSY (50 ms DIPSI-3, 9.7 kHz B_1) of Oxaldie-3 (5.9 mM in H_2O ; pH 5.4; 30°C) showing random coil-like chemical shifts and limited dispersion of chemical shifts.

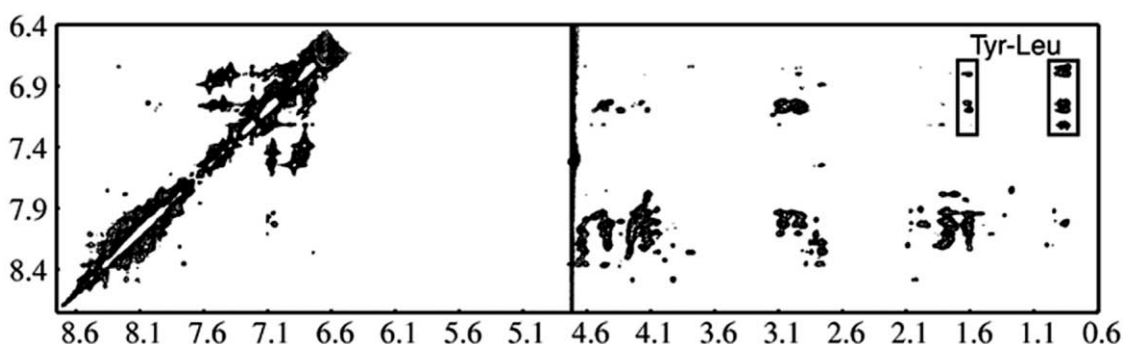


Figure 5. Partial NOESY (200 ms τ_m) spectrum of Oxaldie-3 (5.9 mM in H_2O ; pH 5.4; 30 °C). Significant inter-residue NOE cross peaks are observed between the side chain resonances of tyrosine and leucine residues and for unresolved H_N-H_N contacts. Almost all other cross peaks between amide and aliphatic 1H resonances derive from intra-residue NOEs.

proline-rich helix or between the subunits of the dimer. In addition, CD spectroscopy indicated that a significant amount of Oxaldie-3 was in the α -helical conformation. Together these observations suggest that, unlike its bovine homologue,¹⁹ aPP might adopt a molten globule-like conformation in solution.

Kinetics of the Oxaldie-3 catalysed decarboxylation reaction

Rates for the Oxaldie-3 catalysed decarboxylation of oxaloacetate to produce pyruvate were measured by following the conversion of NADH to NAD^+ in the lactate dehydrogenase mediated transformation of pyruvate to lactate. Oxaldie-3 catalysed the decarboxylation of oxaloacetate with Michaelis–Menten kinetics ($k_{cat} = 5.16 \text{ min}^{-1}$; $K_M = 49.4 \text{ mM}$) (Table 1). In contrast to Oxaldie-2, where a concentration of 200 μM was needed for optimal activity, both K_M and k_{cat} were independent of the concentration of Oxaldie-3 between 2 and 200 μM . The catalytic efficiency of Oxaldie-2 was reduced 2-fold by reducing its concentration to 100 μM .⁵ For smaller concentrations Oxaldie-2 displayed a catalytic activity similar to that observed for simple amines as a consequence of its random coil-like structure. The introduction of an active site for the decarboxylation of oxaloacetate into the scaffold of aPP generated a polypeptide, which acts as a catalyst at a 100-fold reduced concentration compared to Oxaldie-2. The catalytic activity of Oxaldie-3 depended on the cluster of lysine residues in the α -helix; replacing the lysine residues with those found in wild-type aPP reduced the catalytic activity by two orders of magnitude.

Interestingly, Oxaldie-3 not only performed its catalytic function at lower concentrations than Oxaldie-2, but it was generally a better catalyst ($k_{cat} = 86.0 \times 10^{-3} \text{ s}^{-1}$; $K_M = 49.4 \text{ mM}$). Under optimal conditions, the Michaelis constants were similar for both catalysts, but the turnover number was more than 10 times bigger for Oxaldie-3. The catalytic efficiency (k_{cat}/K_M) was $1.74 \text{ M}^{-1} \text{ s}^{-1}$ for Oxaldie-3 and only $0.153 \text{ M}^{-1} \text{ s}^{-1}$ for Oxaldie-2. While with simple amines elimination of water from the high-energy carbinolamine intermediate is the slow step in the catalysed decarboxylation of oxaloacetate, analysis of the kinetic data for Oxaldie-1 and -2 revealed that

imine formation was no longer rate determining.⁵ Oxaldie-3 was active at smaller concentrations of catalyst than Oxaldie-2, but the catalytic mechanism was similar. Like Oxaldie-2, it uses conformational energy of its polypeptide fold to force the active site lysine into an environment where its activity is enhanced, and Coulombic binding interactions between the cationic polypeptide and the substrate to lower the energy of the transition state following carbinolamine. However, because imine formation is no longer rate determining, a step following imine formation between oxaloacetate and Oxaldie-3 must have been speeded by one order of magnitude. Tyr (21) lies amidst the lysine cluster and its presence could change the solvation of the ‘active site’ thereby speeding decarboxylation.

In conclusion, Oxaldie-3 showed the characteristics of a pancreatic polypeptide-like structure according to CD spectroscopy and size-exclusion chromatography. Despite adopting a molten globule-like structure in solution, Oxaldie-3 was an efficient catalyst for the decarboxylation of oxaloacetate at concentrations as low as 2 μM , two orders of magnitude lower than for the first generation Oxaldies. It appeared to speed the formation of the protonatable imine intermediate as well as the actual decarboxylation reaction. Relative to

Table 1. Kinetic data for the decarboxylation of oxaloacetate with Oxaldie-2,⁵ Oxaldie-3 and with simple amines^a

Catalyst	[Cat] (μM)	k_{cat}/K_M ($\text{M}^{-1} \text{ s}^{-1}$)	k_{cat} ($\times 10^{-3} \text{ s}^{-1}$)	K_M (mM)
Oxaldie-2 ^b	200	0.153	7.5	48
Oxaldie-2 ^b	100	0.071	15	210
Oxaldie-3	5–40	1.74	86	49.4
Gly-CONH ₂	—	0.011		
Bu-NH ₂ ^c	—	0.0005		
Spont.			0.013	

^aAll parameters were determined at 25 °C in 50 mM BES (pH 7) containing 10 mM NaCl (150 mM NaCl; 1 M NaCl¹³). Reaction rates were measured by monitoring the production of pyruvate using lactate dehydrogenase and following the conversion of NADH to NAD^+ spectrophotometrically at 340 nm.

^bOxaldie-2 is $\text{NH}_2\text{LeuAlaLysLeuLeuLysAlaLysLeuLeuLysLysCONH}_2$; Gly-CONH₂ is glycine amide.

^cBu-NH₂ is butylamine and BES is *N,N*-bis [2-hydroxyethyl]-2-aminoethanesulfonic acid.

simple amines, Oxaldie-3 speeded the decarboxylation of oxaloacetate by more than three orders of magnitude, which is not insignificant when compared to the 8 orders of magnitude of catalysis observed with acetoacetate decarboxylase. Future design efforts must focus on the production of catalysts with well-defined, stable tertiary structure and on speeding the actual decarboxylation following imine formation.

Acknowledgements

This work was supported by a BBSRC grant (RKA) and by the School of Chemistry. We thank Dr. Peter R. Ashton for help with mass spectrometry, Dr. Mark Bycroft (MRC-Centre for Protein Engineering, Cambridge) for help with the interpretation of the NMR data, Dr. Lesley A. Tannahill for critical reading of the manuscript and the members of our laboratory for discussions.

References and Notes

1. Kirby, A. J. *Acta Chem. Scand.* **1996**, *50*, 203.
2. MacBeath, G.; Hilvert, D. *Chem. Biol.* **1996**, *3*, 433.
3. Schultz, P. G.; Lerner, R. A. *Science* **1995**, *269*, 1835.
4. Bartel, D. P. In *The RNA World* (2nd Ed.); Gesteland, R. F., Chech, T. R., Atkins, J. F., Eds.
5. Johnson, K.; Allemann, R. K.; Widmer, H.; Benner, S. A. *Nature* **1993**, *365*, 530.
6. Broo, K. S.; Brive, L.; Ahlberg, P.; Baltzer, L. *J. Am. Chem. Soc.* **1997**, *119*, 11362.
7. Kennan, A. J.; Haridas, V.; Severin, K.; Lee, D. H.; Ghadir, M. R. *J. Am. Chem. Soc.* **2001**, *123*, 1797.
8. Corey, M. J.; Corey, E. *Proc. Natl. Acad. Sci. U.S.A.* **1996**, *93*, 11428.
9. Hamilton, G. A.; Westheimer, F. H. *J. Am. Chem. Soc.* **1959**, *81*, 2277.
10. Hamilton, G. A.; Westheimer, F. H. *J. Am. Chem. Soc.* **1959**, *81*, 6332.
11. Westheimer, F. H. *Tetrahedron* **1995**, *51*, 3.
12. Allemann, R. K. Thesis ETH No. 8804, 1989.
13. Johnsson, K. Thesis ETH No. 9974, 1992.
14. Blondelle, S. E.; Pérez-Paya, E.; Dooley, C. T.; Pinilla, C.; Houghten, R. A. *Trends Analyt. Chem.* **1995**, *14*, 83.
15. Pérez-Paya, E.; Houghten, R. A.; Blondelle, S. E. *J. Biol. Chem.* **1996**, *271*, 4120.
16. Wood, S. P.; Pitts, J. E.; Blundell, T. L.; Tickle, I. J.; Jenkins, J. A. *Eur. J. Biochem.* **1977**, *78*, 119.
17. Blundell, T. L.; Pitts, J. E.; Tickle, I. J.; Wood, S. P.; Wu, C.-W. *Proc. Natl. Acad. Sci. U.S.A.* **1981**, *78*, 4175.
18. Glover, I. D.; Barlow, D. J.; Pitts, J. E.; Tickle, I. J.; Blundell, T. L.; Tatemoto, K.; Kimmel, J. R.; Wollmer, A.; Strassburger, W.; Zhang, Y.-S. *Eur. J. Biochem.* **1985**, *142*, 379.
19. Li, X.; Sutcliffe, M. J.; Schwartz, T. W.; Dobson, C. M. *Biochemistry* **1992**, *31*, 1245.
20. Chang, P. J.; Noelken, M. E.; Kimmel, J. R. *Biochemistry* **1980**, *19*, 1844.
21. Noelken, M. E.; Chang, P. J.; Kimmel, J. R. *Biochemistry* **1980**, *19*, 1838.
22. Greenfield, N.; Fasman, G. D. *Biochemistry* **1969**, *8*, 4108.
23. Wüthrich, K. *NMR of Proteins and Nucleic Acids*; Wiley: New York, 1986.
24. Haezebrouk, P.; Joniau, M.; Vandeal, H.; Hooke, S. D.; Woodruff, N. D.; Dobson, C. M. *J. Mol. Biol.* **1995**, *246*, 382.
25. Ptitsyn, O. B. *Trends Biochem. Sci.* **1995**, *20*, 376.